A 406-year non-growing season precipitation reconstruction in the southeastern Tibetan Plateau

Maierdang Keyimu[1,2], Zongshan Li[1]*, Bojie Fu[1], Guohua Liu[1], Weiliang Chen[1], Zexin Fan[3], Keyan Fang[4], Xiuchen Wu[5], Xiaochun Wang[6]

[1]State Key Laboratory of Urban and Regional Ecology, Research Center for Eco-Environmental Sciences, Chinese Academy of Sciences, Beijing 100085, China

[2]Xinjiang Key Laboratory of Desert Plant Roots Ecology and Vegetation Restoration, Xinjiang Institute of Ecology and Geography, Chinese Academy of Sciences, Urumqi 830011, China

[3]Xishuangbanna Tropical Botanical Garden, Chinese Academy of Sciences, Mengla 666303, China

[4]Key Laboratory of Humid Subtropical Eco-Geographical Process (Ministry of Education), College of Geographical Sciences, Fujian Normal University, Fuzhou 350007, China

[5]State Key Laboratory of Earth Surface Processes and Resource Ecology, Beijing Normal University, Beijing 100875, China

[6]College of Forestry, Northeast Forestry University, Harbin 150040, China

Correspondence to: Zongshan Li (zsli_st@rcees.ac.cn)

Abstract. Trees record climatic conditions during their growth, and tree rings serve as proxy to reveal the features of the historical climate of a region. In this study, we collected tree-ring cores of forest hemlock (*Tsuga forrestii*) from the northwestern Yunnan area of the southeastern Tibetan Plateau (SETP), and created a residual tree-ring width (TRW) chronology. An analysis of the relationship between tree growth and climate revealed that precipitation during the non-growing season (NGS) (from November of the previous year to February of the current year) was the most important constraining factor on the radial tree growth of forest hemlock in this region. In addition, the influence of NGS precipitation on radial tree growth was relatively uniform over time (1956–2005). Accordingly, we reconstructed the NGS precipitation over the period spanning from A.D. 1600–2005. The reconstruction accounted for 28.5% of the actual variance during the common period 1956–2005. Based on the reconstruction, NGS was extremely dry during the years A.D. 1656, 1694, 1703, 1736, 1897, 1907, 1943, 1982, and 1999. In contrast, the NGS was extremely wet during the years A.D. 1627, 1638, 1654, 1832, 1834–1835, and 1992. Similar variations of the NGS precipitation reconstruction series and Palmer Drought Severity Index (PDSI) reconstructions of early growing season from surrounding regions indicated the reliability of the present reconstruction. A comparison of the reconstruction with Climate Research Unit (CRU) gridded data revealed that our reconstruction was representative of the NGS precipitation variability of a large region in the SETP. Our study provided with the first historical NGS precipitation

29 reconstruction in the SETP which enriches the understanding of the long-term climate variability of this region. The NGS
30 precipitation showed slightly increasing trend during the last decade which might accelerate regional forest hemlock growth.

31 **Keywords**: Tree rings; Non-growing season precipitation; Reconstruction; Southeastern Tibetan Plateau

1 Introduction

33 Unravelling the past climate often relies on proxy records. As a widely used proxy material, tree rings provide an opportunity
34 to obtain long-term climate data (Fritts, 1976; Esper et al., 2002; D'Arrigo et al., 2005; Li et al., 2011; Büntgen et al., 2011,
35 2016; Cai et al., 2014; Yang et al., 2014; Schneider et al., 2015; Wilson et al., 2016; Keyimu et al., 2021). These long-term
36 records enable us to identify the inter-annual, decadal and multi-decal variability of historical climatic conditions. They also
37 provide a reference to better understand the nature of current climatic conditions (warming/cooling, drying/wetting) and to
38 project the future regional climate, as well as the dynamic response of earth processes (e.g., forest growth, glacier
39 retreat/advance, stream flow, drought frequency, and forest fires) to climate change.

40 Being the "third pole" of the Earth, the Tibetan Plateau (TP) (average 4000 m a.s.l.) is particularly sensitive to climate change
41 and is one of the fastest warming places in the world (Chen et al., 2020). The average decadal temperature increase at the TP
42 is 0.33°C, which is higher than the world's average decadal temperature increase of 0.20°C (Yan and Liu, 2014). Because of
43 its geographical extent and position within the global circulation system, the TP plays a key role in regional and global
44 atmospheric circulation patterns (Griessinger et al., 2017), not only affecting the mid-latitude westerlies, but also influencing
45 the Asian monsoon circulation through its thermo-dynamical feedbacks (Duan et al., 2006; Rangwala, 2009; Wu et al., 2015).

46 There are large areas of coniferous forest distributed at high altitudes in the southeastern Tibetan Plateau (SETP). Due to
47 their age and relative lack of disturbance they are a source of proxy material (tree rings) that can be used to reveal the past
48 climatic conditions in this region (Bräuning and Mantwill, 2004; Fan et al., 2009; Fang et al., 2010; Li et al., 2011; Wang et
49 al., 2015; Li and Li., 2017; Shi et al., 2017; Huang et al., 2019; Shi et al., 2019; Keyimu et al., 2021). Many
50 dendroclimatological reconstructions of hydroclimatic variables have also been conducted in the SETP (Fan et al., 2008; Zhang
51 et al., 2015; Wernicke et al., 2015; Griessinger et al., 2017; Li et al., 2017; He et al., 2018). However, few studies have focused
52 on the reconstruction of precipitation history (He et al., 2012; Wernicke et al., 2015). The non-growing season (NGS) of
53 vegetation (from November of the previous year to February of the current year) includes the winter monsoon and pre-summer
54 monsoon seasons in the SETP, and water availability during the NGS might therefore have a constraining effect on radial tree
55 growth (Linderholm and Chen, 2005). It is important to understand the long-term precipitation variations during the NGS to
56 evaluate the current trend of precipitation variation and estimate its future patterns, and to determine the future responses of
57 the forest ecosystem under the changing precipitation trend. To our knowledge, however, there have been no reports of the

reconstruction of NGS precipitation in this area. This hinders our understanding of NGS variability from a long-term perspective.

In this study, we collected tree-ring cores of forest hemlock from the Xinzhu Village of northwestern Yunnan in the SETP. The main objectives of the present study were to (1) develop a new tree-ring chronology and identify the responses of forest hemlock radial growth to climate in the investigation area, (2) reconstruct the historical NGS precipitation and evaluate the recent NGS precipitation change in the long-term context, (3) validate the reliability of the reconstruction. Our results not only enrich the historical hydro-climatic information available in the SETP, but also provide with basis to understand the current trend of regional NGS precipitation variation, which is relevant for evaluating the future development of regional forest ecosystem.

2 Materials and methods

2.1 Study area and sampling sites

Tree-ring core samples were collected from Xinzhu Village in Lijiang County in northwestern Yunnan. The sample site was in the Hengduan Mountains in the SETP (Fig. 1). The climate of the study area is regulated by a westerly circulation and the monsoon circulations of the Indian and Pacific oceans. "Hengduan" means "transverse" in the Chinese language, which implies that the mountains in this region lie in the transverse direction from south to north, and the area is a passageway for the Indian monsoon to flow in and climb up to the TP and other parts of the mainland. The SETP is susceptible to monsoon flow and atmospheric circulations (Bräuning and Mantwill, 2004). According to the Weixi meteorological station of the China Meteorological Administration, which was the closest station to our sampling site, the mean annual precipitation was 953 mm from 1955 to 2016. Most of the annual precipitation (Nearly 70%) concentrated in the monsoon season from May to October in this region (Fig. 2), and thus, tree growth is usually constrained by water availability during non-growing season. The coldest temperature was -2.9°C in January and the warmest temperature was 18.6°C in July. The topography of the sampling area is relatively steep, and it is not in favor of the soil development, hence, thin soil layer of alpine meadow soil (Chinese soil taxonomy) covers the bedrock. Forest hemlock is the dominant tree species of the sampling site, and its tree-ring cores were collected from trees which are healthy and relatively isolated, an optimal condition for maximizing climate signals in tree rings (Li et al., 2017). The elevation of the sampling site was 2,966 m a.s.l. A total of 48 tree-ring cores were extracted from 48 trees using a 5.1 mm diameter increment borer. We have used one sampling per tree method to improve the spatial representativity of radial tree growth. Sampling was conducted along an axis perpendicular to the slope inclination to avoid the impact of tension wood (Keyimu et al., 2020).
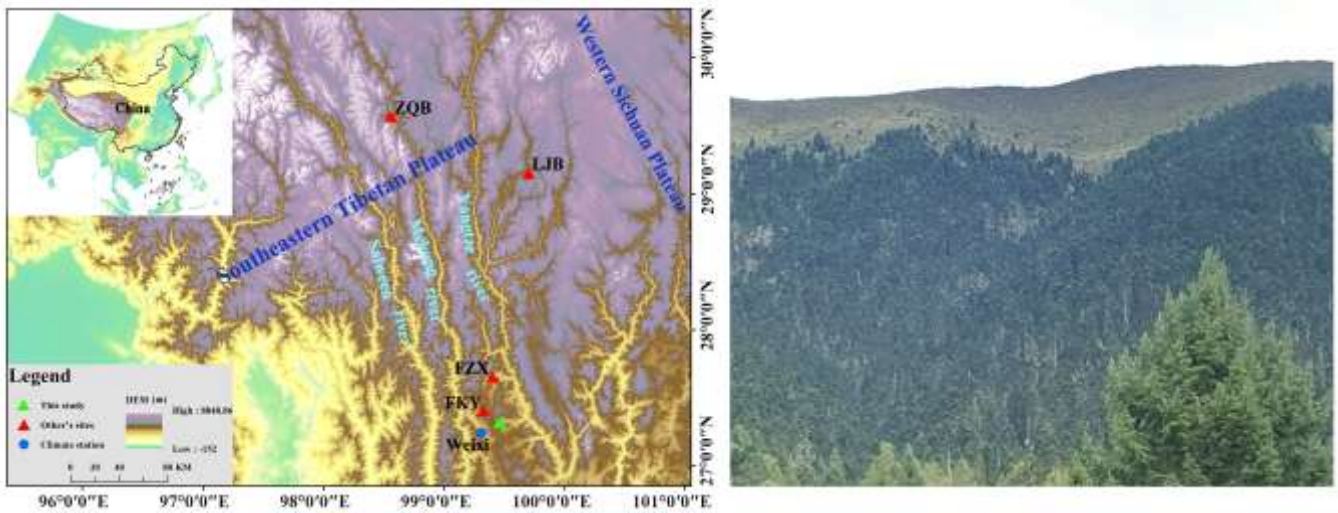
86

87 **Figure 1:** Map of the study area. The green triangle is the study site. The red triangles are the sites in other studies (previous year May –

88 current year April PDSI reconstruction site in Fang et al., 2010; current year March – May PDSI reconstruction site in Fan et al., 2008;

89 current year April – June PDSI reconstruction site in Li et al., 2017; current year May – June PDSI reconstruction site in Zhang et al., 2015).

90 The blue dot is the meteorological station in Weixi County. On the right is the landscape image of tree ring sampling site.

91
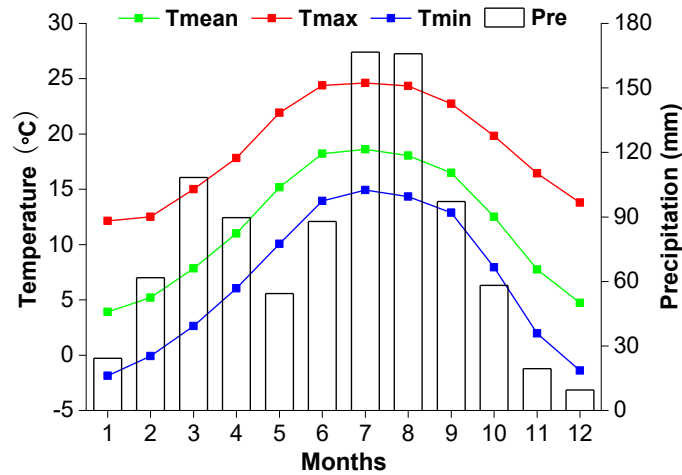
92

93 **Figure 2**: The ombrothermic diagram of the climate variables in the study area

94 **2.2 Establishment of the tree-ring chronology**

95 The tree-ring samples were treated with standard dendrochronological procedures. They were first glued onto wooden holders

96 and air-dried, and then polished to a flat surface with sand paper until the tree rings were clearly visible. The LINTAB 6.0 tree

97 ring measurement system was used to measure the tree-ring width (TRW). We have marked the tree rings of each sample at

98 each ten-year interval and visually checked the tree ring pattern matching among samples, then confirmed the crossdating

99 quality using the COFFECHA program (Holmes, 1983). Thirty-eight of the tree-ring cores were adopted for a further analysis

100 after excluding the bad quality samples and the un-crossdated samples. The tree-ring series was detrended with a negative

101 exponential model to remove the age dependency of tree growth (Cook et al., 1995). We have used the residual chronology

102 since it removes the auto-correlation in tree ring growth and captures high frequent climate signal. The "dplR" software toolkit

103 (Bunn, 2018) within the R software environment (R Core Team 2020) was used for detrending and chronology establishment.

104 The reliable period of the chronology was determined based on the criterion of expressed population signal (EPS) > 0.85

105 (Wigley, 1984).

106 **2.3 Climate data**

107 Temperature and precipitation records were obtained from the Weixi meteorological station (27.17° N, 99.28° E, 2326 m a.s.l.)

108 operated by the China Meteorological Administration. Data was available for the period of 1955–2005. Climate data (including

109 the maximum, minimum and average temperatures, and precipitation) were provided by the China Meteorological Data

110 Sharing Service Platform. A self-calibrated Palmer Drought Severity Index (scPDSI) was downloaded from the 3.26e gridded

111 dataset of the Climate Research Unit (CRU) via the Royal Netherlands Meteorological Institute (KNMI) climate explorer (data

112 accessed on 23rd December, 2020, data re-accessed for the updated version (CRU scPDSI 4.05 early) of PDSI data on 20th of

113 April, 2021) using the coordinates of the tree ring sampling site. The range of CRU grid box is 27.0 – 27.5° N, 99.0 – 99.5° E.

114 **2.4 Tree growth and climate relationship analysis**

115 We analysed the relationship between climate and tree growth using Dendroclim 2002 software (Biondi and Waikul, 2004).

116 Pearson correlation values and response function values were calculated for the relationships between TRW indices and climate

117 variables for the period of 1955–2005. Due to the carry over effect of the climatic conditions of the previous-year on the current

118 year tree growth (Fritts, 1976), the tree growth – climate relationship analysis spanned a 16-month period from June of the

119 previous year to September of the current year. We also used the seasonalised climate variables because it made more eco-

120 physiological sense for growth than single months. To observe the temporal stability of the climate influence on radial tree

121 growth, we conducted a moving correlation analysis at a moving interval of 32 years. All the correlation results were considered

122 significant at the 95% confidence level.

123 **2.5 Statistics of chronology and climate reconstruction**

124 We have used the expressed population signal (EPS) to determine the reliable period of the chronology; mean inter-series

125 correlation (Rbar), signal-to-noise ratio (SNR) and variance of first eigenvector (VFE) to evaluate the common signal among

126 measurement series; standard deviation (SD) and mean sensitivity (MS) to show the degree of inter-annual variability of the

127 chronology. According to the analysis of the relationship between the TRW indices and constraining climatic factors, we
128 developed a linear regression model (Cook and Kairiukstis, 1990) for the climate reconstruction. As in many other tree ring
129 based climate reconstructions, we tested the goodness-of-fit of the model using the leave-one-out cross-validation method
130 (Michaelsen, 1987). We used the Pearson's correlation coefficient (r), explained variance (R^2), adjusted explained variance
131 (R_{adj}^2), reduction of error (RE), sign test (ST), coefficient of efficiency (CE), and product mean test (Pmt) to evaluate the
132 fidelity of the reconstruction model (Fritts et al., 1990).

133 3. Results

134 3.1 Characteristics of the TRW chronology

135 Residual TRW chronology of forest hemlock from the investigation area was established (Fig. 3). The descriptive statistics of
136 the chronology were presented in Table 1. According to the criteria of EPS > 0.85, the most reliable length of the TRW
137 chronology was 406 years (A.D. 1600–2005). The mean correlation among tree-ring series (Rbar) was 0.48, and the variance
138 in the first eigenvector (VFE) was 27 %, which implied a relatively strong common signal among individual trees constituting
139 the chronology. The relatively low inter-annual variability of the chronology was expressed by the small mean sensitivity value
140 (0.23). The EPS and SNR values (average EPS and SNR were 0.89 and 6.87 for the total length chronology, respectively)
141 further implied the existence of the common signal among each individual measurement series. In general, all the statistical
142 parameters indicated the potential climate signal imprinted in our TRW chronology.
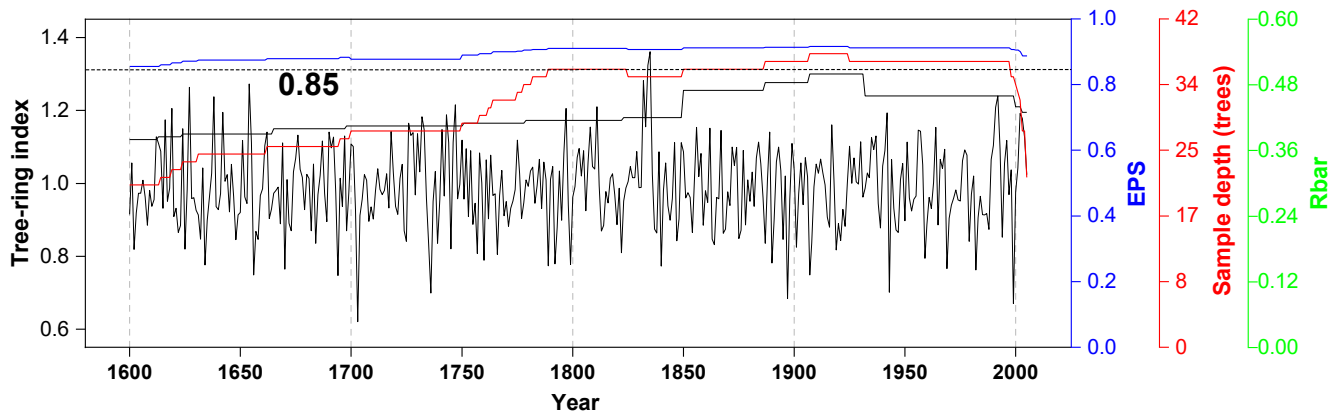
143

144 **Figure 3:** Plot of tree-ring residual chronology, the running inter-correlations among cores (Rbar, the green line), expressed population
145 signal (EPS, the blue line) and the sample size (the red line). The Rbar and EPS were calculated using a 30-year window, with a 15-year lag.
146 The horizontal dashed line denotes the EPS threshold level (0.85).

147

Table 1. Site information, chronology statistics and results of a common interval span analysis of residual tree-ring width (TRW) chronology from the Xinzhu Village, northwestern Yunnan in China

Type	Location	Elevation (m)	Time length	Number of cores	SD	MS	Rbar	SNR	EPS	VFE
Tree ring	99.43°E, 27.25°N	2966	1600–2005	38	0.22	0.23	0.48	6.87	0.89	0.27

Note: SD: standard deviation, MS: mean sensitivity, Rbar: mean inter-series correlation, SNR: signal-to-noise ratio, EPS: Expressed Population Signal, VFE: Variance in first eigenvector.

3.2 Tree growth and climate relationship analysis

According to the results of the tree growth and climate relationship analyses (Fig. 4), the precipitation during the NGS was the most important constraining factor ($R = 0.56$, $p < 0.001$) on the radial growth of forest hemlock in the study area. The results of a response function analysis further confirmed the strong correlation between NGS precipitation and forest hemlock radial growth. The results of a moving correlation analyses between TRW chronology and instrumental NGS precipitation record (Fig. 5) were positively significant (at 99%) during the investigated period (1956-2005), indicating that the NGS precipitation influence was stationary over time.

159
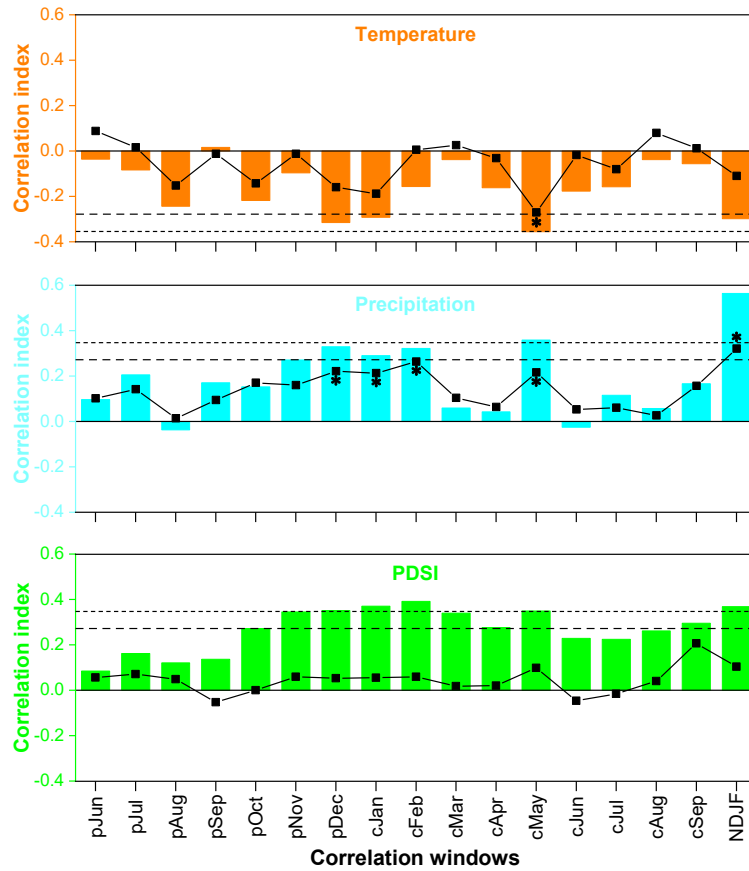
Figure 4: Correlations between tree-ring indices and temperature, precipitation, and scPDSI in the correlation windows from previous year June to current year September, as well as in NDJF (non-growing season, NGS) for the common period from 1956 to 2005. The horizontal dashed and dotted lines indicate the threshold of the correlations at the 95% and 99% significance levels. Black line with squares denotes the results of response function analysis between tree-ring indices and climate variables. The asterisks next to the squares denote the significant effects ($p < 0.05$) of response function analyses.

165
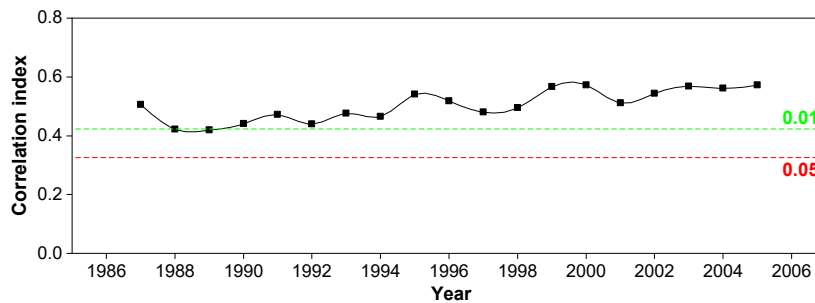
 Figure 5: The moving correlation result between tree-ring width (TRW) chronology and non-growing season (NGS) precipitation during

167 the period of 1956–2005. The horizontal red and green dashed lines denote the significance levels of 0.05 and 0.01, respectively.

168 **3.3 Non-growing season precipitation reconstruction**

169 According to the relationship between the TRW chronology and NGS precipitation, we developed a linear regression model

170 ($y = 229.94x$-109.45 mm) and reconstructed the historical NGS precipitation series, which extended back to A.D. 1600 (Fig.

171 6b). In the model, y is the NGS precipitation, and x is the TRW index. The reconstruction accounted for 28.5% of the

172 instrumental NGS precipitation variability during the common time span (1956–2005). Figure 6a shows the similarities

173 between the instrumental and reconstructed NGS precipitation series. We used a leave-one-out cross-verification method to

174 evaluate the legitimacy of the reconstruction model (Table 2). The positive RE and CE values (0.18 and 0.15, respectively)

175 were indicative of legitimacy of the reconstruction. The significant value (at 95%) of sign test implied that the model predicted

176 values were generally in line with the variation trend of instrumental values. In addition, the significant values of F test (at

177 99%) and PM test (at 95%) further confirmed the validity of the reconstruction. Overall, the statistics indicated that the

178 reconstruction model possessed good predictive skills.
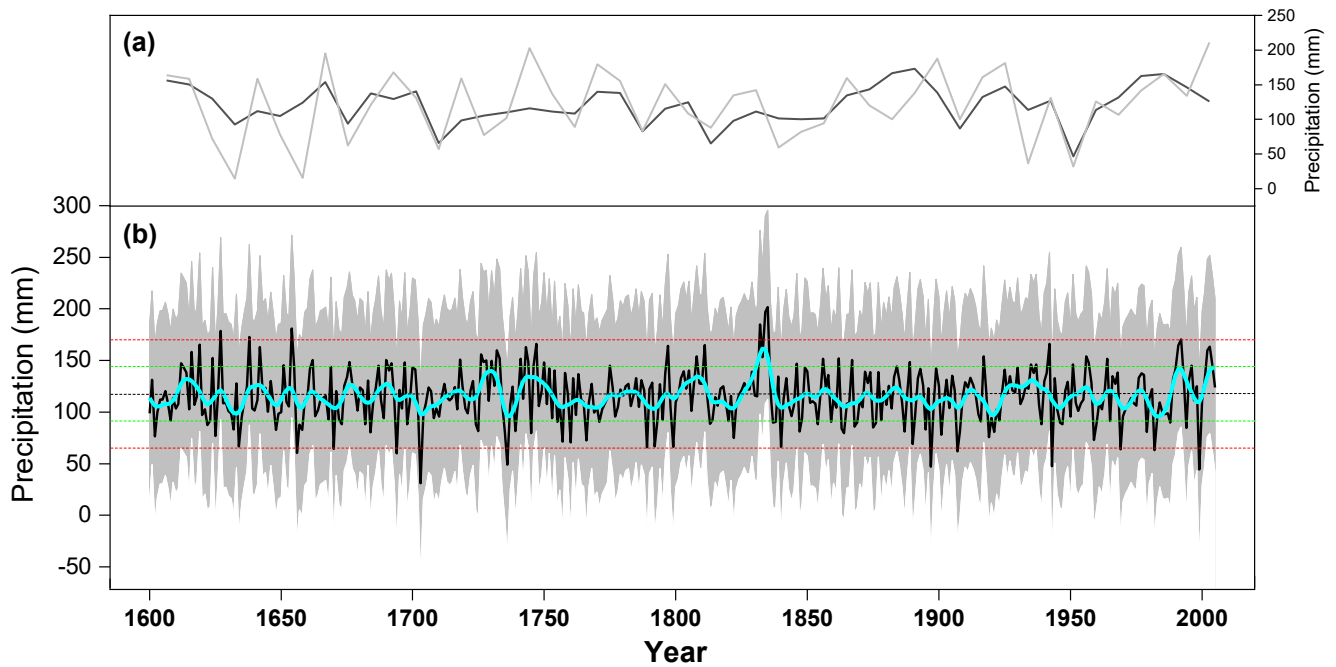
179

180 **Figure 6:** Non-growing season (NGS) precipitation reconstruction from A.D. 1600 to 2005. (a) The black line is the

181 reconstruction series, the thick cyan line is the 11- year loess smoothed series. The horizontal black dashed line is the mean of

182 NGS precipitation value during from A.D. 1600–2005. The horizontal green and red dashed lines are the one time and two

183 times the of standard deviations of NGS precipitation, which demonstrated the boundaries of dry and extremely dry (below
184 mean), and wet and extreme wet (above mean) years. The grey shading indicated the 95% confidence interval of the
185 reconstruction; (b) Instrumental (black) and reconstructed (grey) NGS precipitation during their common period of 1956–2005.

186 **Table 2. Leave-one-out verification statistics for the non-growing season (NGS) precipitation reconstruction**

	R	R^2	R_{adj}^2	F	Sign-test	Pmt	RE	CE
Calibration	0.561	0.315	0.285	–	–	–	–	–
Verification	0.524	0.274	0.235	18.6**	36+/13−*	7.89*	0.18	0.15

187 Note: R correlation coefficient, R^2 explained variance, R_{adj}^2 is the adjusted explained variance, F F-test, Sign-test sign of paired observed
188 and estimated departures from their mean on the basis of the number of agreements/disagreements, Pmt product mean test, RE reduction of
189 error, CE coefficient of efficiency. * $p < 0.05$, ** $p < 0.01$

3.4 Characteristics of the NGS precipitation reconstruction

191 Figure 6b shows the reconstructed NGS precipitation over the past 406 years (A.D. 1600–2005). The mean of the reconstructed
192 NGS precipitation series was 118 mm, and the standard deviation (SD) was 26 mm. We pre-defined the years that had NGS
193 precipitation above 144 mm (mean+SD) as wet NGS years, and above 170 mm (mean+2SD) as extremely wet years (Table
194 3), whereas we defined years that had precipitation below 92 mm (mean-SD) as dry NGS years, and below 66 mm (mean-2SD)
195 as extremely dry NGS years (Table 3). The dry/wet periods and some of the extreme dry/wet NGS periods in the present
196 reconstruction were synchronised with dry/wet periods and extreme dry/wet periods in previously reported PDSI
197 reconstruction from the surrounding region (Fig. 7, Table S2, Table S3), though some dissimilarities were also existed. As
198 shown in Fig. 8, the instrumental (**a, c**) and reconstructed (**b, d**) NGS precipitation series could represent the climatic conditions
199 over a similar area in the SETP.

200

Table 3 Extreme wet and dry NGS years

Year	Dry (mm)	Year	Wet (mm)
1656	63	1627	181
1694	62	1638	175
1703	33	1654	183
1736	51	1832	187
1897	49	1834	199
1907	64	1835	204
1943	50	1992	173
1982	65		
1999	47		
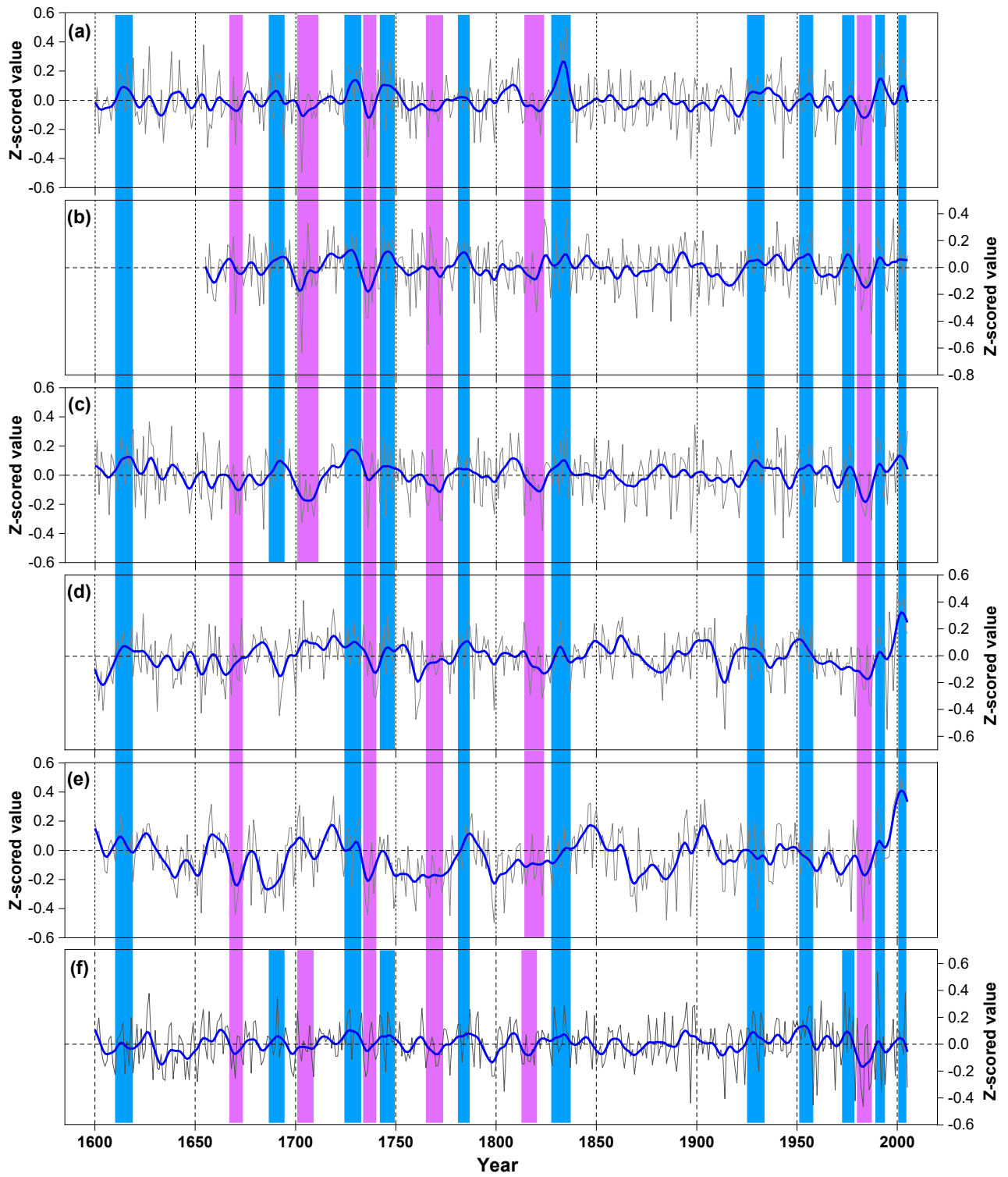
202 **Figure 7:** Comparisons of the hydroclimatic reconstructions in different studies. (a) The non-growing season (NGS)
203 precipitation reconstruction in the present study. (b) The current year March – May average Palmer Drought Severity Index
204 (PDSI) reconstruction in Fan et al. (2008). (c) The reconstruction of average PDSI from May of the previous year to April of
205 the current year in Fang et al. (2010). (d) The current year May-June average PDSI reconstruction in Zhang et al. (2015). (e)
206 The current year April-June average PDSI reconstruction in Li et al. (2017). (f) drought series extracted from Asian Monsoon
207 Atlas from the nearest point (Cook et al. 2010). The blue and purple bars show the common wet and dry periods of the different
208 reconstructions, respectively.
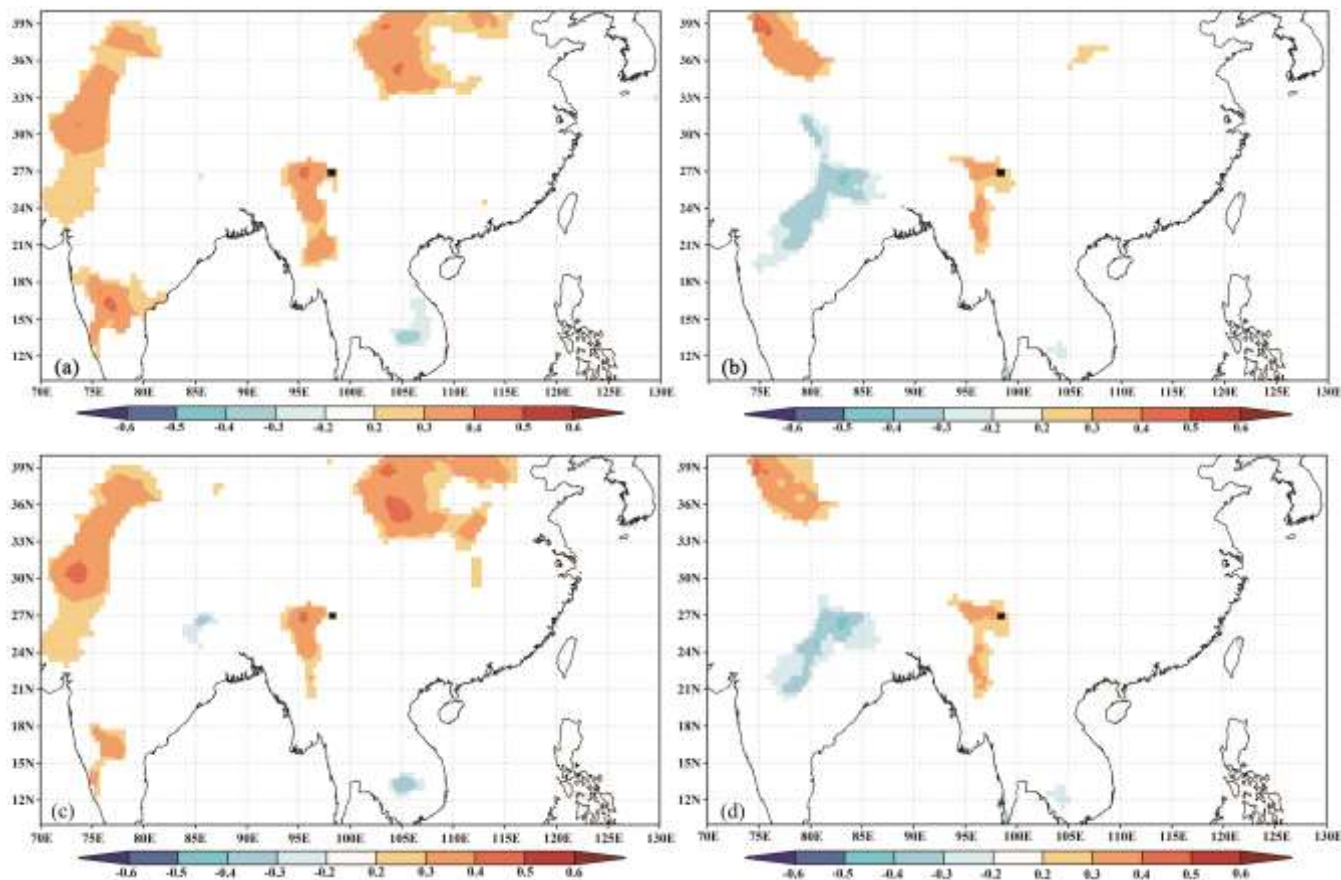
211 **Figure 8:** Spatial correlations of actual (a: raw data; c: first-differenced data) and reconstructed (b: raw data; d: first-differenced
212 data) non-growing season (NGS) precipitation with a gridded dataset of the NGS precipitation (average from November of the
213 previous year to February of the current year) during their overlapping periods (1956–2005). The black square indicates the
214 location of the study site.

4. Discussion

4.1 Tree growth and climate relationship

The results of the tree growth and climate relationship analyses suggested that the forest hemlock radial growth in the northwestern Yunnan region of the SETP was strongly constrained by hydroclimatic factors. According to the Pearson correlation analysis, the influence of precipitation during the NGS on radial tree growth was greater than that of any other investigated climate variables and any correlation window. The response function analysis further confirmed the strong impact of NGS precipitation. In addition, the results of 32-year interval of moving correlation analysis (Fig. 5) suggested the temporally consistent influence of NGS precipitation on forest hemlock radial growth in this region. The importance of NGS precipitation on the radial tree growth could be attributed to the fact that precipitation during the NGS compensated for the soil moisture, which was crucially important for supporting tree growth in the following season (Linderholm and Chen, 2005; Treydte et al. 2006; Wu et al., 2019; Li et al., 2021). This is because tree growth is often water stressed in the early stages of its growth in each year on the SETP when the monsoon precipitation does not arrive (Bräuning and Mantwill, 2004; Zhang et al., 2015), and the earlywood of tree rings mainly use spring melt water (Zhu et al., 2021). The eco-physiological importance of NGS precipitation on tree growth and tree water usage was also revealed by isotope ratios method-based investigations. Brinkmann et al's (2018) study showed that nearly 40% of the uptaken water by *Fagus sylvatica* and *Picea abies* trees in a temperate forest of middle Europe are sourced from NGS precipitation. Tree-ring oxygen isotope ratios ($\delta^{18}O$) are demonstrated to contain NGS precipitation signals in the Himalayan region (Huang et al., 2019; Zhu et al., 2021). Huang et al's (2019) study revealed that NGS precipitation (snowfall) increased the snow-depth and the later snowmelt compensated soil moisture in the spring and early summer, which was a crucially important water source for the Juniper growth in the southwestern Tibetan Plateau. Zhu et al's (2021) investigation in the western Himalaya revealed that formation of earlywood in tree rings of *Pinus wallachina* depended on the snowmelt originated from NGS precipitation. The weak influence of precipitation on regional forest hemlock growth during March and April and strong influence during May was connected with the saddle-shaped monthly rainfall pattern of this area (Fig. 2). The highest correlation between precipitation and TRW chronology was observed in May of the current year. This is because the xylogenous activity to form earlywood coincided with the low precipitation in this month (Fig. 2). In addition, the melt water was probably used up (tree uptake + evaporation) during the early spring. Therefore, water stressed was increased during the late spring (May). The correlations between precipitation and the TRW chronology were not significant during the growing season (June-September) because an adequate water supply was available in the summer monsoon season.

Precipitation during the NGS over the SETP falls as snow. According to Sommerfeld et al. (1993) and Stadler et al. (1996), the development of a snowpack insulates the underlying soil from freezing temperatures, which creates unfrozen soil conditions and most of the soil processes that are active during warmer conditions also persist under snow cover, albeit at a reduced rate (Edwards, 2007). Unfrozen soil can reduce the cold and frost damage to the shallow root systems of conifer trees

247 in this region (Schenk and Jackson, 2002). A reduction in the cold damage to roots decreases the energy required to form new

248 roots in the following growth year (Pederson et al., 2004), with the saved energy potentially used to initiate xylogenesis and

249 form earlywood cells. Evergreen tree species are known to carry out year-round photosynthetic activity (Oquist and Huner,

250 2003; Prats and Brodersen, 2020), albeit at a slower rate during the NGS, and therefore, the higher moisture availability

251 contributes to the carbohydrate and energy accumulation process of forest hemlock in the investigation area.

252 In contrast, the radial tree growth was negatively correlated to temperature in most correlation windows (Fig. 4). This can

253 be explained by the fact that higher temperature enhances evapotranspiration, and thus decreases water availability, which

254 eventually constrains tree growth. The negative impact of NGS temperature on radial tree growth was obvious because the

255 strengthened evaporation due to higher temperatures might reduce the moisture compensation to the soil layer and cause water

256 stress during the early stage of the following growth season.

257 **4.2 Validity of the reconstructed precipitation series**

258 We have tried to validate the fidelity of the newly reconstructed series from different aspects. Although we used the residual

259 TRW chronology in the present study, which removes autocorrelation (Cook and Kairiukstis, 1990) to capture the high

260 frequency climate signals as in Fan et al. (2008) and Chen et al. (2016), the variability of dry and wet NGS at different scales

261 was still retained in the reconstructed series. The reconstructed series in the present study demonstrated the variation in dry

262 and wet NGS years (Fig. 6b). As in many other proxy based historical climate reconstruction studies, we compared our NGS

263 precipitation series with other hydroclimatic reconstructions from the surrounding areas to investigate the reliability of our

264 reconstruction. However, there was no reported historical NGS precipitation record in the SETP, and we had to compare the

265 present reconstruction series with available hydro-climatic reconstructions, e.g., PDSI. There are only countable numbers of

266 PDSI reconstructions in the nearby region. Hence, we could only compare the present NGS precipitation reconstruction with

267 existing PDSI reconstructions (Fig. 7) which are of spring or early summer. Dry/wet climate during these seasons are usually

268 associated with the winter precipitation, hence, it makes certain sense to carry out the comparison. The correlation coefficients

269 between our NGS precipitation reconstruction and the PDSI reconstructions of Fan et al. (2008), Fang et al. (2010), Zhang et

270 al. (2015) and Li et al. (2017) were 0.51 (n = 702), 0.35 (n = 1062), 0.25 (n = 1062) and 0.22 (n = 1016) ($p < 0.001$). We have

271 extracted the drought series of Asian Monsoon Atlas (Cook et al.2010) from the nearest point to our investigation site and

272 compared it with the NGS precipitation reconstruction in present study ($R = 0.35$, n = 1062, $p < 0.001$). As can be observed

273 from Fig. 7, there were dry and wet periods in compared reconstruction series which were consistent with the NGS precipitation

274 variabilities. These similarities indicated the reliability of our NGS precipitation reconstruction to some extent. The correlation

275 coefficients for the present reconstruction with those of Fan et al. (2008) and Fang et al. (2010) were greater than those with

276 Li et al. (2017) and Zhang et al. (2015). These differences were probably due to the different distances among the study sites.

277 Although, the major dry and wet periods were similar in the hydroclimatic reconstructions referenced above, there were still

278 certain discrepancies in duration and the strength of the dry/wet climatic conditions. This is probably because of the differences

279 in the types of hydroclimatic variables (precipitation, PDSI), specific seasons reconstructed (annual, seasonal), tree species
280 (species with different drought tolerances), chronology recording methods (standard chronology, residual chronology), length
281 of calibration period, sample replication and the geomorphic differences of the tree ring sampling sites (altitude, slope) (Table
282 S1).

283 In addition, we uploaded both of the instrumental and reconstructed NGS precipitation data for the same period of 1956–
284 2005 on the KNMI website and conducted a spatial correlation analysis with the CRU gridded climate dataset. The similar
285 patterns of spatial correlation between the instrumental and reconstructed data and their first differenced data (Fig. 8) indicated
286 that the present reconstruction was reliable and could represent the NGS precipitation over a large area in the SETP. Besides,
287 the occurrence of some historical great drought events in the Asian monsoon area (Cook et al., 2010, Kang et al., 2013), i.e.,
288 the 1756–1768 (strange parallels drought), 1790, 1792–1796 (east India drought) and 1920s (China mega-drought), matched
289 the dry NGS periods in our reconstruction, which also further confirmed the reliability of our reconstruction.

5. Conclusion

291 In this study, we investigated 406 years of residual TRW chronology of forest hemlock in the SETP, China. The climate and
292 tree growth relationship analyses showed that the TRW chronology was mostly negatively correlated with the thermal variable
293 (temperature), whereas it was positively correlated with hydroclimatic variables (precipitation) and PDSI, indicating that
294 hydroclimatic conditions determined the radial growth of forest hemlock in this region. Accordingly, we derived a linear model
295 of the relationship between climate and tree growth, which accounted for 28.5% of the actual NGS precipitation variance
296 (1956–2005), and we used the model to reconstruct the historical (A.D. 1600–2005) NGS precipitation. The reconstructed
297 series showed that the NGS was extremely dry during the years A.D. 1656, 1694, 1703, 1736, 1897, 1907, 1943, 1982 and
298 1999. In contrast, the NGS was extremely wet during the years A.D. 1627, 1638, 1654, 1832, 1834–1835 and 1992. A
299 comparison between the NGS precipitation reconstruction in this study and PDSI reconstructions from nearby regions revealed
300 a coherency in the timing of dry and wet episodes, suggesting the reliability of our reconstruction. Our results showed that the
301 NGS precipitation demonstrated slightly increasing trend since 1980s which is in favor of the future forest ecosystem
302 development. In the future, more efforts should be made to collect wide-area of tree-ring data and develop more proxy
303 chronologies that will enable us to reveal historical precipitation variability at the longer and wider scale in the SETP.

304 **Data availability**. The climate reconstruction series in this study can be obtained from Zongshan Li after the paper publication.

305 **Author contributions**. ZSL and MK conceived the study; ZSL, ZXF, XCW collected the tree-ring data; MK, ZSL, ZXF, KYF,
306 XCW elaborated the methodology; MK, ZSL, WLC analysed the data; MK, ZSL led the writing of the manuscript; ZSL and
307 ZXF revised the manuscript; BJF and GHL validated the final manuscript.

308 **Competing interests**. The authors declare that they have no conflict of interest.

309 **Acknowledgement**. This work was funded by the National Key Research Development Program of China (2016YFC0502105),

310 the second Tibetan Plateau Scientific Expedition and Research (STEP) Program (2019QZKK0502). We are grateful to the

311 editor and anonymous reviewers for their valuable comments and suggestions to improve this article.

References

313 Biondi. F. and Waikul, K.: DENDROCLIM2002: a C++ program for statistical calibration of climate signals in tree ring

314 chronologies, Comput. Geosci., 30(3), 303-311, https://doi.org/10.1016/j.cageo.2003.11.004, 2004

315 Bräuning, A. and Mantwill, B.: Summer temperature and summer monsoon history on the Tibetan Plateau during the last 400

316 years recorded by tree rings, Geophys. Res. Lett., 31, L24205, https://doi.org/10.1029/2004GL020793, 2004

317 Bunn, A. G. and Korpela, M.: An introduction to dplR. The Comprehensive R Archive Network,

318 https://cran.biodisk.org/web/packages/dplR/vignettes/intro-dplR.pdf, 2018

319 Büntgen, U., Myglan, V. S., Ljungqvist, F. C., McCormick, M., Di Cosmo N., Sigl, M., Jungclaus, J., Wagner, S., Krusic, P.

320 J., Esper, J., Kaplan, J. O., de Vaan MAC., Luterbacher, J., Wacker, L., Tegel, W. and Kirdyanov, A. V.: Cooling and societal

321 change during the Late Antique Little Ice Age from 536 to around 660 AD, Nat. Geosci., 9, 231–236,

322 https://doi.org/10.1038/ngeo2652, 2016

323 Büntgen, U., Tegel, W., Nicolussi, K., McCormick, M., Frank, D., Trouet, V., Kaplan, J. O., Herzig, F., Heussner, K. U.,

324 Wanner, H., Luterbacher, J. and Esper, J.: 2500 years of European climate variability and human susceptibility, Science, 331,

325 578–582, https://doi.org/10.1126/science.1197175, 2011

326 Cai, Q. F, Liu, Y., Lei, Y., Bao, G. and Sun, B.: Reconstruction of the march-august PDSI since 1703 AD based on tree rings

327 of Chinese pine (*Pinus tabulaeformis* Carr.) in the Lingkong Mountain, southeast Chinese loess Plateau, Clim. Past., 10, 509–

328 521, https://doi.org/10.5194/cp-10-509-2014, 2014

329 Chen, F., Yuan, Y. J, Zhang, T. W, Shang, H.: Precipitation reconstruction for the northwestern Chinese Altay since 1760

330 indicates the drought signals of the northern part of inner Asia, Int. J. Biometeorol., 60(3), 455-463.

331 https://doi.org/10.1007/s00484-015-1043-5, 2016

332 Cook, E. R. and Kairiukstis, A.: Methods of Dendrochronology: Applications in the Environmental Sciences, Kluwer

333 Academic Press, Dordrecht, 1990

334 Cook, E. R., Anchukaitis, K. J., Buckley, B. M., D'Arrigo, R. D., Jacoby, G. C. and Wright, W. E.: Asian monsoon failure and

335 megadrought during the last millennium, Science, 328(5977), 486-489, https://doi.org/10.1126/science.1185188, 2010

336 Cook, E. R., Briffa, K. R., Meko, D. M., Graybill, D. A. and Funkhouser, G.: The 'segment length curse' in long tree-ring

337 chronology development for palaeoclimatic studies, Holocene, 5(2), 229-237. https://doi.org/10.1177/095968369500500211,

338 1995

339 D'Arrigo, R. D., Mashig, E., Frank, D. C., Wilson, R. J. S. and Jacoby, G. C.: Temperature variability over the past millennium

340 inferred from Northwestern Alaska tree rings, Clim. Dynam., 24, 227-236. https://doi.org/10.1007/s00382-004-0502-1, 2005

341 Duan, K., Yao, T. and Thompson, L.: Response of monsoon precipitation in the Himalayas to global warming, J. Geophys.

342 Res., 111, D19110. https://doi.org/10.1029/2006JD007084, 2006

343 Edwards, A. C., Scalenghe, R., Freppaz, M.: Changes in the seasonal snow cover of alpine regions and its effect on soil

344 processes: a review. Quat. Int., 162-163, 172-181. https://doi.org/10.1016/j.quaint.2006.10.027, 2007

345 Esper, J.: 1300 years of climatic history for Western Central Asia inferred from tree rings, Holocene, 12(3), 267-277.

346 https://org.doi.10.1191/0959683602hl543rp, 2002

347 Fan, Z. X., Bräuning, A. and Cao, K. F.: Tree-ring based drought reconstruction in the central Hengduan Mountains region

348 (China) since AD 1655, Int. J. Climatol., 28, 1879–1887, https://doi.org/10. 1002/joc.1689, 2008

349 Fan, Z. X., Bräuning, A., Yang, B. and Cao, K. F.: Tree ring density-based summer temperature reconstruction for the central

350 Hengduan Mountains in southern China, Glob. Planet. Change, 65 (1-2), 1-11. https://doi.org/10.1016/j.gloplacha.2008.10.001,

351 2009

352 Fang, K. Y, Gou, X. H, Chen, F., Li, J. B., D'Arrigo, R., Cook, E. D, Yang, T. and Davi, N.: Reconstructed droughts for the

353 southeastern Tibetan Plateau over the past 568 years and its linkages to the Pacific and Atlantic Ocean climate variability,

354 Clim. Dyn., 35(4), 577–585. https://doi.org/10.1007/s00382-009-0636-2, 2010

355 Fritts, H. C., Guiot, J. and Gordon, G. A.: Verification. In: Cook E and Kairiukstis LA, eds., Methods of Dendrochronology:

356 Applications in the Environmental Sciences. Dordrecht, Kluwer Academic Publishers, 178-184, 1990

357 Fritts, H. C.: Tree rings and climate. Academic Press, London, 1976

358 Griessinger, J., Bräuning, A., Helle, G., Hochreuther, P. and Schleser, G.: Late Holocene relative humidity history on the

359 southeastern Tibetan plateau inferred from a tree ring $\delta^{18}O$ record: recent decrease and conditions during the last 1500 years,

360 Quat. Int., 430, 52–59, http://dx.doi.org/10.1016/j.quaint.2016.02.011, 2017

361 He, H. M., Bräuning, A., Griessinger, J., Hochreuther, P. and Wernicke, J.: May–June drought reconstruction over the past

362 821 years on the southcentral Tibetan Plateau derived from tree-ring width series, Dendrochronologia, 47, 48–57,

363 https://doi.org/10.1016/j.dendro.2017.12.006, 2018

364 He, H. M., Yang, B., Bräuning, A., Wang, J. L. and Wang, Z. Y.: Tree-ring derived millennial precipitation record for the

365 south-central Tibetan plateau and its possible driving mechanism, Holocene, 23 (1), 36-45,

366 https://doi.org/10.1177/0959683612450198, 2012

367 Holmes, R. L.: Computer-assisted quality control in tree-ring dating and measurement, Tree-ring Bulletin, 43, 69-75, 1983

Huang, R., Zhu, H. F., Liang, E. Y., Liu, B., Shi, J. F., Zhang, R. B., Yuan, Y. J., Griessinger, J.: A tree ring-based winter temperature reconstruction for the southeastern Tibetan Plateau since 1340 CE, Clim. Dyn., 53, 3221-3233. https://doi.org/10.1007/s00382-019-04695-3, 2019

Kang, S. Y, Bao, Y., Qin, C., Wang, J. L, Feng, S., Liu, J. J.: Extreme drought events in the years 1877–1878, and 1928, in the southeast Qilian mountains and the air–sea coupling system. Quat. Int., 283(427), 85-92. https://doi.org/10.1016/j.quaint.2012.03.011, 2013

Keyimu, M., Li, Z. S., Liu, G. H., Fu, B. J., Fan, Z. X., Wang, X. C. Zhang, Y. D., Halik, U.: Tree-ring based minimum temperature reconstruction on the southeastern Tibetan Plateau, Quat. Sci. Rev., 251, 106712. https://doi.org/10.1016/j.quascirev.2020.106712, 2021

Keyimu, M., Wei, J. S., Zhang, Y. X., Zhang, S., Li, Z. S., Ma, K. M., Fu, B. J.: Climate signal shift under the influence of prevailing climate warming – Evidence from *Quercus liaotungensis* on Dongling Mountain, Beijing, China, Dendrochronologia, 60, 125683. https://doi.org/10.1016/j.dendro.2020.125683, 2020

Li, J. B., Shi, J. F., Zhang, D. D., Yang, B., Fang, K. Y. and Yue, P. H.: Moisture increase in response to high-altitude warming evidenced by tree-rings on the southeastern Tibetan Plateau, Clim. Dyn., 48, 649–660. https://doi.org/10.1007/s00382-016-3101-z, 2017

Li, T., Li, J.B.: A 564-year annual minimum temperature reconstruction for the east central Tibetan Plateau from tree rings, Glob. Planet. Change, 157, 165-173. https://doi.org/10.1016/j.gloplacha.2017.08.018, 2017.

Li, Z. S., Zhang, Q. B. and Ma, K. P.: Tree-ring reconstruction of summer temperature for A.D. 1475–2003 in the central Hengduan Mountains, northwestern Yunnan, China, Clim. Change, 110(1-2), 455-467, https://doi.org/10.1007/s10584-011-0111-z, 2011

Linderholm, H. W., Chen, D.: Central Scandinavian winter precipitation variability during the past five centuries reconstructed from *Pinus sylvestris* tree rings, Boreas, 34, 43–52, https://doi.org/10.1080/03009480510012845, 2005

Michaelsen, J.: Crossevalidation in statistical climate forecast models, J Clim. App. Meteorol., 26, 1589-1600, 1987

R: A language and environment for statistical computing. R Foundation for Statistical Computing, Vienna, Austria. URL https://www.R-project.org/., 2020

Oquist, G., Huner, N. P.: Photosynthesis of overwintering evergreen plants, Annu. Rev. Plant Biol., 54, 329–355. https://doi.org/10.1146/annurev.arplant.54.072402.115741, 2003

Prats, K. A., Brodersen, C. R.: Seasonal coordination of leaf hydraulics and gas exchange in a wintergreen fern, AoB Plants, 12(6), 1–13. https://doi.org/10.1093/aobpla/plaa048, 2020

Pederson, N., Cook, E. R., Jacoby, G. C., Peteet, D. M., Griffin, K. L.: The influence of winter temperatures on the annual radial growth of six northern range margin tree species, Dendrochronologia, 22 (1), 7–29. https://doi.org/10.1016/j.dendro.2004.09.005, 2004

Rangwala, I., Miller, J. R. and Xu, M.: Warming in the Tibetan Plateau: Possible influences of the changes in surface water vapor, Geophys. Res. Lett., 36, L06703, https://doi.org/10.1029/2009GL037245, 2009

Schenk, H. J., & Jackson, R. B.: The global biogeography of roots. Ecol. Monogr., 72, 311–328. https://doi.org/10.1890/0012-9615(2002)072[0311:TGBOR]2.0.CO;2, 2002

Schneider, L., Smerdon, J. E., Büntgen, U., Wilson, R. J. S., Myglan, V. S., Kirdyanov, A. V. and Esper, J.: Revising mid-latitude summer temperatures back to AD 600 based on a wood density network, Geophys. Res. Lett., 42, 4556-4562. https://doi.org/10.1002/2015GL063956, 2015

Shi, C. M., Sun, C., Wu, G. C., Wu, X. C., Chen, D. L., Masson-Delmotte, V., Li, J. P., Xue, J. Q., Li, Z. S., Ji, D. Y., Zhang, J., Fan, Z. X., Shen, M. G., Shu, L. F., Ciais, P.: Summer temperature over Tibetan Plateau modulated by Atlantic multi-decadal variability, J. Clim., 32, 4055-4067. https://doi.org/10.1175/JCLI-D-17-0858.1, 2019

Shi, S. Y., Li, J. B., Shi, J. F., Zhao, Y. S. and Huang, G.: Three centuries of winter temperature change on the southeastern Tibetan plateau and its relationship with the Atlantic Multidecadal Oscillation, Clim. Dyn., 49, 1305-1319. https://doi.org/10.1007/s00382-016-3381-3, 2017

Sommerfeld, R. A., Mosier, A. R., Musselman, R. C.: CO_2, CH_4 and N_2O flux through a Wyoming snowpack and implications for global budget, Nature, 361, 140–142, https://doi.org/10.1038/361140a0, 1993

Stadler, D., Wunderli, H., Auckenthaler, A., Fluhler, H.: Measurement of frost induced snowmelt runoff in a forest soil, Hydrol. Process., 10, 1293–1304, https://doi.org/10.1002/(SICI)1099-1085(199610)10:10<1293::AID-HYP461>3.0.CO;2-I, 1996

Wang, J. L., Yang, B., Ljungqvist, F. C.: A millennial summer temperature reconstruction for the eastern Tibetan Plateau from tree-ring width, J. Clim., 28(13), 5289-5304. https://doi.org/10.1175/JCLI-D-14-00738.1, 2015

Wernicke, J., Griessinger, J., Hochreuther, P., Bräuning, A.: Variability of summer humidity during the past 800 years on the eastern Tibetan plateau inferred from $\delta^{18}O$ of tree-ring cellulose. Clim. Past, 10(4), 3327-3356. https://doi.org/10.5194/cp-11-327-2015. 2015

Wigley, T. M., Briffa, K. R., and Jones, P. D.: On the average value of correlated time series, with applications in dendroclimatology and hydrometeorology, J. Clim. Appl. Meteorol., 23, 201–213, https://doi.org/10.1175/1520-0450(1984)0232.0.CO;2, 1984

Wilson, R., Anchukaitis, K., Briffa, K. R., Büntgen, U., Cook, E., D'Arrigo, R., Davi, N., Esper, J., Frank, D., Gunnarson, B., Hegerl, G., Helama, S., Klesse, S., Krusic, P.J., Linderholm, H.W., Myglan, V., Osborn, T.J., Rydval, M., Schneider, L.,

427 Schurer, A., Wiles, G., Zhang, P. and Zorita, E.: Last millennium northern hemisphere summer temperatures from tree rings:
428 Part I: the long-term context, Quat. Sci. Rev., 134, 1-18. https://doi.org/10.1016/j.quascirev.2015.12.00, 2016

429 Wu, G., Duan, A., Liu, Y., Mao, J., Ren, R., Bao, Q., He, B., Liu, B. and Hu, W.: Tibetan Plateau climate dynamics: recent
430 research progress and outlook, Natl. Sci. Rev., 2, 100–116, https://doi.org/10.1093/nsr/nwu045, 2015

431 Wu, X. C., Li, X. Y., Liu, H. Y., Ciais, P., Li, Y. Q., Xu, C. Y., Babst, F., Guo, W. C., Hao, B. Y., Wang, P., Huang, Y. M.,
432 Liu, S. M., Tian, Y. H., He, B. and Zhang, C. C.: Uneven winter snow influence on tree growth across temperate China, Glob.
433 Change Biol., 25, 144–154. https://doi.org/10.1111/gcb.14464, 2019

434 Yan, L. and Liu, X.: Has climatic warming over the Tibetan Plateau paused or continued in recent years? J. Earth Ocean Atmos.
435 Sci., 1, 13–28, 2014

436 Yang, B., Qin, C., Wang, J., He, M., Melvin, T. M., Osborn, T. J.: A 3,500-year tree-ring record of annual precipitation on the
437 northeastern Tibetan Plateau, Proc. Natl. Acad. Sci. U. S. A., 111(8), 2903-2908. https://doi.org/10.1073/pnas.1319238111,
438 2014

439 Zhang, Q. B., Evans, M. N., Lyu, L. X.: Moisture dipole over the Tibetan Plateau during the past five and a half centuries, Nat.
440 Commun., 6, 8062. https://doi.org/10.1038/ncomms9062, 2015

441 Zhu, H. F., Huang, R., Asad, F., Liang, E. Y., Bräuning, A., Zhang, X. Z., Dawadi, B., Man, W. M., Griessinger, J.: Unexpected
442 climate variability inferred from a 380-year tree-ring earlywood oxygen isotope record in the Karakoram, Northern Pakistan,
443 Clim. Dyn., https://doi.org/10.1007/s00382-021-05736-6, 2021